Journal of Applied Fluid Mechanics, Vol. 11, No. 5, pp. 1193-1199, 2018.
Available online at www.jafmonline.net, ISSN 1735-3572, EISSN 1735-3645.
DOI: 10.29252/jafm.11.05.28149

Periodic Moving Track Analysis of Spiral Oil Wedge Journal Bearing under Dynamic Loading

L. L. Wang [1], Q. L. Zeng[1†], M. Wang[2] and Q. G. Chen [1]

[1] *College of Mechanical and Electronic Engineering, Shandong University of Science and Technology, Qingdao, 266590, China*
[2] *College of Mechanical and Electronic Engineering, China university of Petroleum, Qingdao, 266580, China*

†*Corresponding Author Email: qlzeng@sdust.edu.cn*

(Received June 29, 2017; accepted May 4, 2018)

ABSTRACT

The moving track of journal bearing changes with the time in the condition of dynamic loading. The force balance equation of journal bearing is established, and the generalized Reynolds equation, the oil film thickness equation of spiral oil wedge journal bearing under dynamic loading are gained, which is based on axial inertia force, bearing capacity and dynamically loading. By finite difference method, Euler method and Reynolds boundary condition, the generalized Reynolds equation and force balance equations are solved simultaneously, the periodic moving track of journal bearing at different times is solved. The results show that the circumferential pressure, axis displacement, axis velocity, axis acceleration velocity of journal bearing change periodically as time goes. The influence of dynamical loading on pressure distribution of oil film and axis locus is analyzed.

Keywords: Spiral oil wedge journal bearing; Dynamic loading; Moving track; Force balance equation.

NOMENCLATURE

c	bearing clearance
e_1	eccentricity of eccentric circular surface
e_d	eccentricity of the axial centroid relative to the spin axis
h	oil film thickness
Mg	the weight of the axis
p	oil film pressure
Q_x, Q_y	dynamic loading of axis
R	bearing radius
R_1	radius of circular surface
t	computed time
u_a	journal speed
W_x, W_y	bearing capacity for x and y separately
x	circumferential direction
$\dot{x}$, $\dot{y}$	vertical direction displacement and horizontal direction velocity separately
$\ddot{x}$, $\ddot{y}$	axial instantaneous acceleration
y	radial direction
z	axial direction
α	position angular of eccentric circular surface
ω_a	axis rotating speed
η	fluid dynamic viscosity
Φ	dimensionless circumference coordinates

1. INTRODUCTION

There is a higher demand for the dynamic characteristics of journal bearing with the development of high speed rotating machinery, especially, the transient and cyclical characteristics of bearing axis locus under complex loads have become an important factor affecting the accuracy and stability of rotating machinery. Osman (2014) studied numerically the performance of dynamically loaded finite journal bearing lubricated with non-Newtonian fluid, considering the elastic deformation of bearing. Based on the mass conservation cavitation method, Zhang *et al*. (2000) studied the characteristics of dynamically loaded finite journal bearings by solving the modified Reynolds equation, energy equation and heat conduction equation. Shao *et al*. (2015) analyzed numerically the performance characteristics of engine main bearings under hydrodynamic loads in a six-cylinder in-line diesel engine. Pan *et al*. (2005) and Su (2003) studied experimentally the oil film rupture status of dynamically loaded journal bearings which was the same method with preference (Elord *et al*. 1974), and compared with the theoretical results of incompressible mass-conserving cavitation algorithm. Ma *et al*. (2004;

2006) investigated theoretically the behavior of dynamically loaded journal bearings lubricated with non-Newtonian couple stress fluids and built the cavitation damage model. Ertuğrul *et al.* (2003) investigated the frictional behavior of the engine journal bearings using the theoretical Reynolds equation and experimental test rig. Li *et al.* (2016) identified the oil-film stiffness and damping coefficients based on equivalent load reconstruction. Sawicki *et al.* (2005) presented the transient analysis of submerged journal bearing incorporating the mechanism of shear between the liquid sublayer and air cavity in the cavitation zone. Wang (2011; 2002) computed numerically the performance of dynamically loaded journal bearings lubricated with micropolar fluids and couple stress fluids based on the improved Elord cavitation algorithm and over-relaxation method. Yu *et al.* (2002) compared mobility method with mass conservation method for dynamically loaded journal bearings. Pettinato *et al.* (2001) measured the temperature, eccentricity, attitude angle, circumferential film thickness profiles and dynamic characteristics of a highly preloaded three-lobe bearing. For ultra high rotation speed rolling bearing, the dynamic and thermal stability of bearing cage is the main problem, Yan *et al.* (2016) indicated that the appropriate cage parameters were significant to air-oil flow and thermal dissipation inside bearing cavity. Christiansen *et al.* (2017) investigated the journal orbit of a dynamically loaded journal bearing using the traditional two-dimensional Reynolds equation and three-dimensional Navier-Stokes equations. In this manuscript, by establishing the force balance equation, the oil film thickness equation and the generalized Reynolds equation of spiral oil wedge journal bearing in the condition of dynamical loading, the moving track of spiral oil wedge journal bearing is analyzed using finite difference method, Euler method and Reynolds boundary condition.

2. MATHEMATICS MODEL OF DYNAMIC LOADING CONDITIONS

2.1 Generalized Reynolds equation under dynamic loading

The generalized Reynolds equation of radial journal bearing in the condition of incompressible flow, laminar is as following:

$$\frac{1}{R^2}\frac{\partial}{\partial\phi}(h^3\frac{\partial p}{\partial\phi})+\frac{\partial}{\partial z}(h^3\frac{\partial p}{\partial z})=6u_a\eta\frac{\partial h}{R\partial\phi}+12\eta\frac{\partial h}{\partial t} \quad (1)$$

Where p is oil film pressure, Φ is dimensionless circumference coordinates, η is fluid dynamic viscosity, h is oil film thickness, R is bearing radius, u_a is journal speed, z is axial direction, t is computed time.

Spiral oil wedge journal bearing has three titled spiral oil wedges in the circumferential direction and both ends of every oil wedge have oil feed holes and oil return holes (as shown in Fig. 1). The special structure of journal bearing makes flow characteristics of lubrication change, the lubrication from the oil feed holes 2 flows along oil wedge and leaks out of the bearing from the other oil return holes 1, which realizes the fluid flow separate between the oil wedges.

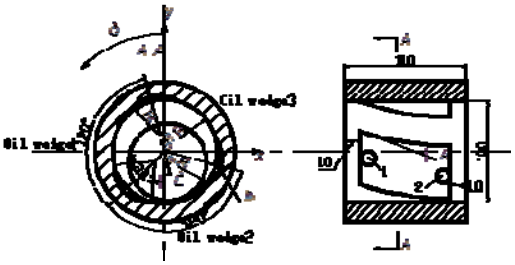

Fig. 1. Structure of spiral oil wedge journal bearing

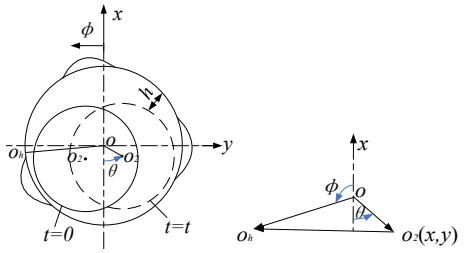

Fig. 2. Oil film thickness diagram at dynamical loading

Figure 2 is the calculation diagram of oil film thickness, O is the bearing center, O_2 is denoted by $(x,y)$and it is axis center, O_h is the calculation location whenφ is rotated along x axis, the triangle ΔOO_hO_2 can be formed by O_h, bearing center O and axis center O_2. OO_2 is eccentricity, $OO_2=e=\sqrt{x^2+y^2}$, $\cos\theta=-x/e$, $\sin\theta=y/e$, θ is attitude angle. The oil film of spiral oil wedge journal bearing is as following:

$$\begin{cases} h=c-x\cos\phi+y\sin\phi & \text{cylinder surface} \\ h=c-x\cos\phi+y\sin\phi+ \\ R_1\sqrt{1-[\frac{e_1\sin(\phi-\alpha)}{R_1}]^2}+ & \text{eccentric circular surface} \\ e_1\cos(\phi-\alpha)-R \end{cases} \quad (2)$$

Whether the computation point position is in cylinder surface or eccentric arc surface, the oil film thickness equation of cylinder surface and eccentric circular surface with the change of time is as following:

$$\frac{\partial h}{\partial t}=-\dot{x}(t)\cos\phi+\dot{y}(t)\sin\phi \quad (3)$$

Where c is bearing clearance, x is circumferential coordinate, y is radial coordinate, R_1 is radius of cylinder surface, e_1 is the eccentricity of the eccentric arc surface, α is the position angular of eccentric arc surface, $\alpha=ztg\beta/R$, $\dot{x}(t)$, $\dot{y}(t)$ are vertical direction velocity and horizontal direction velocity separately.

Substituting Eq. (3) into (1), the generalized

Reynolds equation can be written as follows:

$$\frac{1}{R^2}\frac{\partial}{\partial\phi}\left(h^3\frac{\partial p}{\partial\phi}\right)+\frac{\partial}{\partial z}\left(h^3\frac{\partial p}{\partial z}\right)=6u_a\eta\frac{\partial h}{R\partial\phi} \quad (4)$$
$$+12\eta\left(-\dot{x}(t)\cos\phi+\dot{y}(t)\sin\phi\right)$$

2.2 Force balance equations of axis under dynamic loading

Dynamic loading has periodically unbalanced load, transient load and etc., the axis center O_2 varies with the time under dynamical loading. As shown in Fig. 3, O_2 is axis center and its coordinate is (x, y), O is the bearing center, the force balance computation equations in the horizontal direction and the vertical direction can be expressed as following:

$$\begin{aligned} -M\ddot{x} &= -W_x(\omega_a t)+Q_x+Mg \\ M\ddot{y} &= W_y(\omega_a t)+Q_y \end{aligned} \quad (5)$$

Where W_x, W_y are bearing capacity for x and y separately, Q_x, Q_y are dynamic loading of axis, $Q_x = Me_d\omega_a^2\cos\omega_a t$, $Q_y = Me_d\omega_a^2\sin\omega_a t$, $\ddot{X}$, $\ddot{Y}$ are the axial instantaneous acceleration, Mg is the weight of the axis, ω_a is axis rotating speed, e_d is eccentricity of the axial centroid relative to the spin axis.

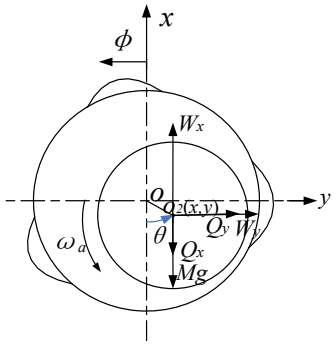

Fig. 3. Dynamic loading calculation model

2.3 Solution of generalized Reynolds equation

The generalized Reynolds Eq. (4) and force balance Eqs. (5) are computed for solving the periodic moving track of journal bearing at different times. The generalized Reynolds equation is computed by finite difference method and Reynolds boundary condition. Firstly, the generalized Reynolds equation of initial time is solved, oil film pressure is derived, the termination of iteration result is judged according to the convergence criterion $\sum_{i=2}^{m}\sum_{j=2}^{n}\left|p_{i,j}^{Ln+1}-p_{i,j}^{Ln}\right| \Big/ \sum_{i=2}^{m}\sum_{j=2}^{n}\left|p_{i,j}^{Ln}\right| \le 10^{-4}$. And then oil film component W_x, W_y are gotten according to oil film pressure, axial instantaneous acceleration $\ddot{X}$, $\ddot{Y}$ are gotten by force balance equation. Finally the next position parameters and velocity parameters are computed according to Euler method and they are introduced into generalized Reynolds equation, oil film pressure of next time is computed. So axis locus at given time t is computed according to the previous similar method.

3. COMPUTED PARAMETERS OF NONLINEAR PERIODIC MOVING TRACK

The main parameters of the bearing are shown as follows: the bearing radius R is 50mm, the bearing width is 110mm, the oil groove width is 90mm, the spiral angle β is 0.6, the oil groove wrap angle is 80º, depth of the arc recess h_0 is 0.12mm, inlet water pressure is 0.3MPa, the viscosity of water η is 0.0013 Pa•s, the density of water is 1000 kg•m^{-3}, the quality of axis M is 20kg, the interval of time is $\pi/100$, the computing time $\bar{t}$ is 15π, rotational speed N is 3000r/min, dynamic eccentricity $\varepsilon_d = \frac{e_d}{c}$ is 0.3, 0.6, 1.

4. RESULTS AND ANALYSIS

4.1 Effect of dynamic loading on oil film pressure

Figures 4, 5 and 6 are circumferential pressure distribution of 6 times in the case of different dynamic eccentricities $\varepsilon_d = 0.3$ (ε_d is equated with exerting a unbalance load on axis), $\varepsilon_d = 0.6$, $\varepsilon_d = 1$ and dimensionless axial coordinate λ=0.2, λ=0.5, λ=0.8 within load variation period. With the change of time, cavitation locations vary periodically, 2pi is a period, the computed time is chosen from 6pi to 8pi. The Figs show that: (1) As time goes, the peak of circumferential pressure, oil film rupture location and reformation location move along the rotation direction of axis, and the maximum of pressure occurs alternately at λ=0.2, λ=0.5, λ=0.8 within load variation period. This is because that the periodic change of dynamic eccentricities leads to periodic pressure. (2) The periodic dynamic load leads that dynamic eccentricities can lie in the convergence and divergence zone, the peak of oil film pressure shows a trend of increases and then decreases. And the peak of pressure increases with the increase of dynamic eccentricities, which is consistent with the following status. Journal bearing produces bigger oil film pressure in order to be in equilibrium with the external loading with the increase of unbalance loading. (3) Circumferential pressure does not produce three pressure strips and produces two pressure strips at most which is not consistent with the change trend of static loading. The reason is as follows: the dynamic load is periodic, especially the dynamic eccentricity plays a leading role compared with oil groove at bigger dynamic eccentricity, and therefore circumferential pressure only produces a pressure strip.

4.1 Effect of dynamic loading on axis position

Figures 7, 8 and 9 are axis equilibrium position in

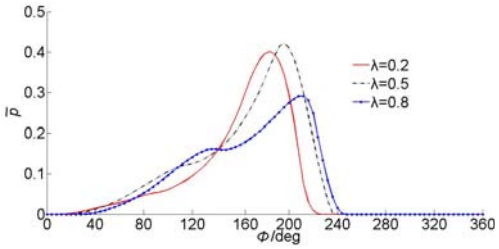

(a) $\bar{t} = 6pi(8pi)$

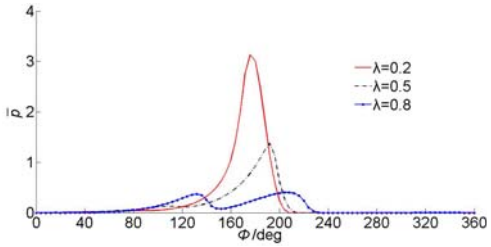

(b) $\bar{t} = 6.4pi$

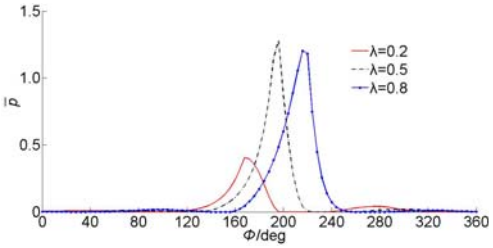

(c) $\bar{t} = 6.8pi$

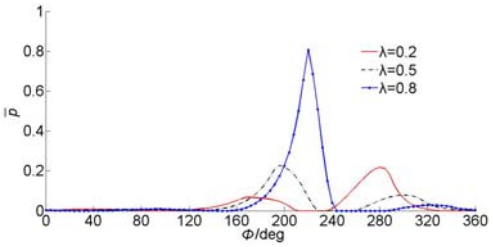

(d) $\bar{t} = 7.2pi$

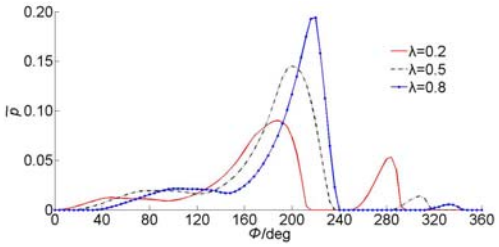

(e) $\bar{t} = 7.6pi$

Fig. 4. Oil film pressure of different times at $\varepsilon_d = 0.3$

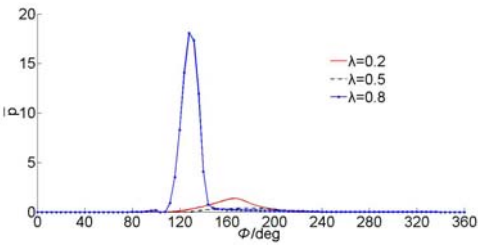

(a) $\bar{t} = 6pi(8pi)$

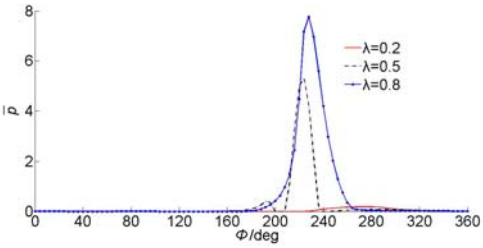

(b) $\bar{t} = 6.4pi$

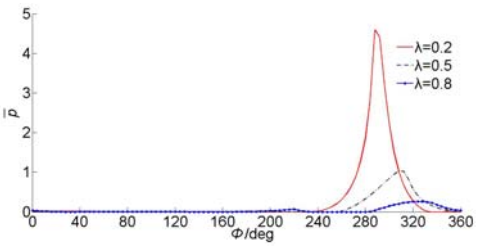

(c) $\bar{t} = 6.8pi$

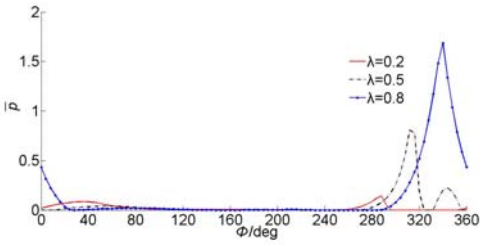

(d) $\bar{t} = 7.2pi$

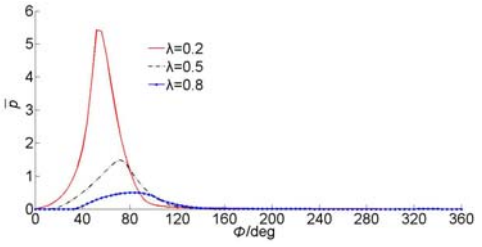

(e) $\bar{t} = 7.6pi$

Fig. 5. Oil film pressure of different times at $\varepsilon_d = 0.6$

the case of different dynamic eccentricities $\varepsilon_d = 0.3$, $\varepsilon_d = 0.6$, $\varepsilon_d = 1$ within load variation period. The Figs show that: (1) The axis orbit is elliptical at different dynamic eccentricities ε_d. (2) With the increase of ε_d, the center of axis orbit is rapidly approaching the coordinate original point, orbit radius increases, ellipticity of bearing decreases and is rapidly approaching circle, which is more obvious at $\varepsilon_d > 0.6$.(3) The radius of curvature is much bigger at bigger disturbance unbalance load, and it is not small displacement whirl. (4) Axis displacement X, Y, axis velocity $\dot{X}$, $\dot{Y}$, axis acceleration velocity $\ddot{X}$, $\ddot{Y}$ vary periodically with the change of time. The amplitude of vibration for axis displacement, axis velocity, axis acceleration velocity is smaller at smaller

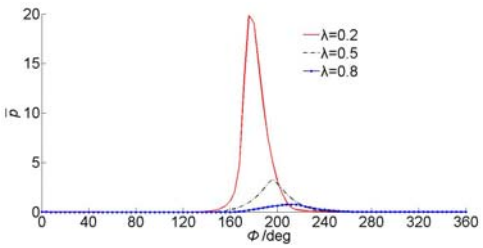

(a) $\bar{t} = 6pi(8pi)$

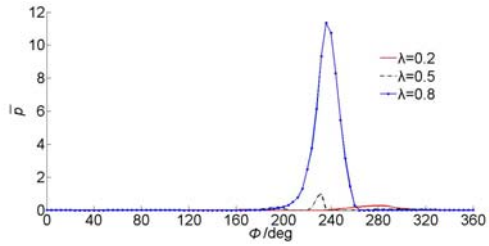

(b) $\bar{t} = 6.4pi$

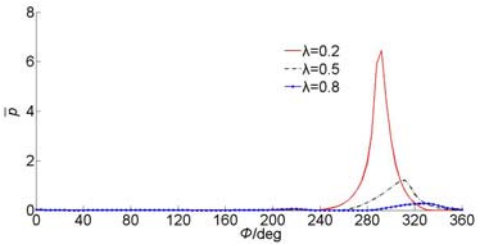

(c) $\bar{t} = 6.8pi$

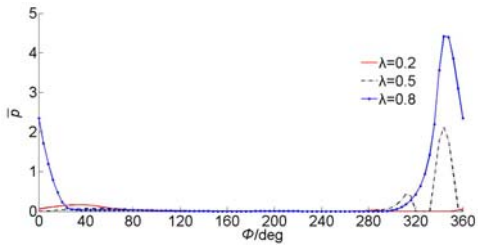

(d) $\bar{t} = 7.2pi$

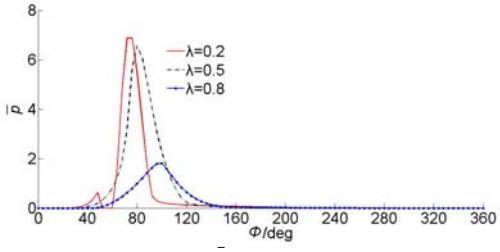

(e) $\bar{t} = 7.6pi$

Fig. 6. Oil film pressure of different times at $\varepsilon_d = 1$

disturbance unbalance load, axis has smaller displacement whirl near the balance position. The amplitude of vibration for journal bearing increases at bigger disturbance unbalance load, the center of axis orbit deviates from the proceeded balance position. Especially, the displacement is rapidly approaching the clearance circle at $\varepsilon_d > 0.6$, which is because that journal bearing increases

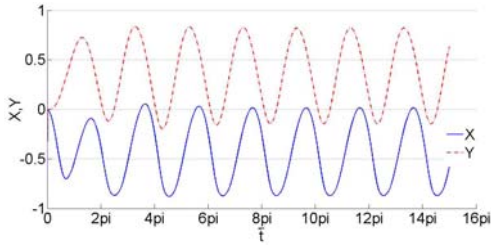

(a) Axis displacement *X, Y*

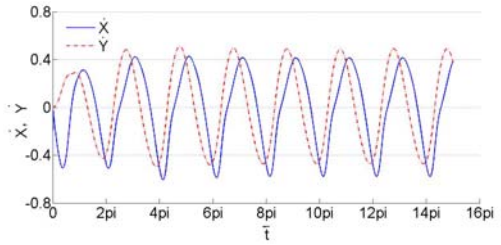

(b) Axis velocity $\dot{X}$ **,** $\dot{Y}$

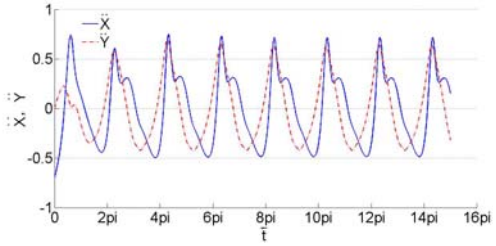

(c) Axis acceleration velocity $\ddot{X}$ **,** $\ddot{Y}$

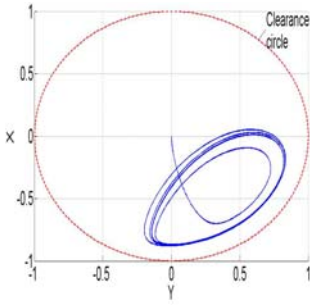

(d) Axis orbit

Fig. 7. Axis position of different times at $\varepsilon_d = 0.3$

eccentricity and produces bigger pressure for balancing with the external load with the increase of unbalance loading.

5. CONCLUSIONS

By solving the force balance equation, oil film thickness equation and Reynolds equation under dynamic loading, the oil film pressure and axis position at different times are analyzed, the main conclusions are as follows:

(1) The oil film thickness equation, Reynolds equation for spiral oil wedge journal bearing under dynamic loading are gained. And axial instantaneous acceleration equation is established, which is based on the force balance of journal inertia force, bearing capacity and dynamical loading.

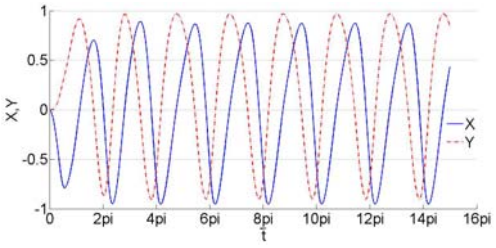

(a) Axis displacement *X, Y*

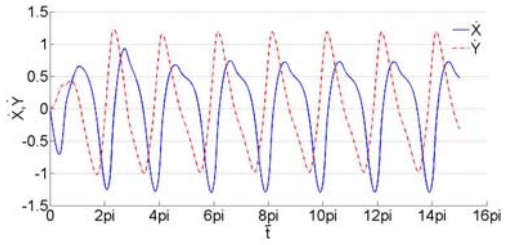

(b) Axis velocity $\dot{X}$, $\dot{Y}$

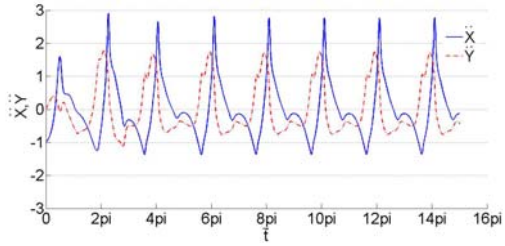

(c) Axis acceleration velocity $\ddot{X}$, $\ddot{Y}$

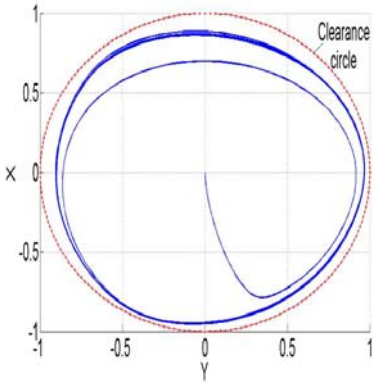

(d) Axis orbit

Fig. 8. Axis position of different times at $\varepsilon_d = 0.6$

(2) As time goes, the peak of circumferential pressure, oil film rupture location and reformation location move along the rotation direction of axis, and the maximum of pressure occurs alternately at different axial locations within load variation period; axis displacement, axis velocity and axis acceleration velocity vary periodically within load variation period.

(3) As dynamic eccentricity increases, the peak of pressure increases, the center of axis orbit is rapidly approaching the coordinate original point, orbit radius increases, ellipticity of bearing decreases and is rapidly approaching circle, the amplitude of vibration for axis displacement, axis velocity and axis acceleration velocity increases.

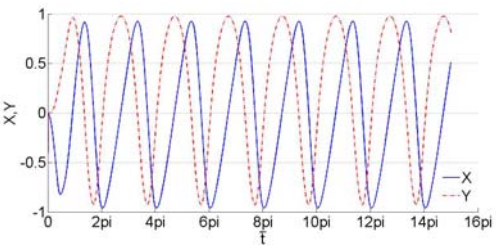

(a) Axis displacement *X, Y*

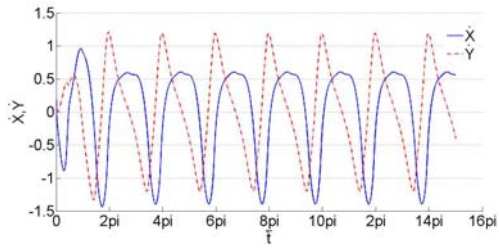

(b) Axis velocity $\dot{X}$, $\dot{Y}$

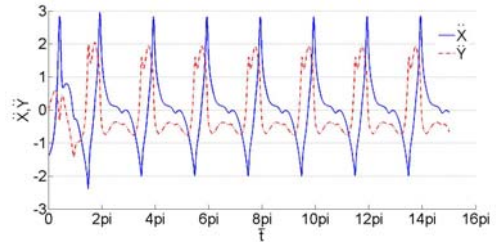

(c) Axis acceleration velocity $\ddot{X}$, $\ddot{Y}$

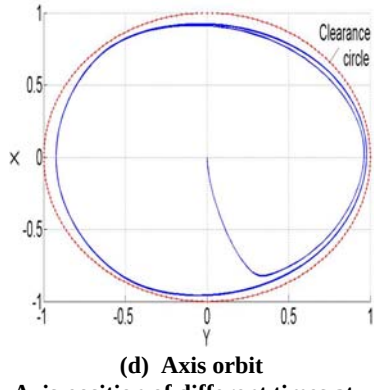

(d) Axis orbit

Fig. 9. Axis position of different times at $\varepsilon_d = 1$

ACKNOWLEDGEMENTS

This work was supported by the grant from China Postdoctoral Science Foundation funded project (No. 2017M612304), Shandong Provincial Postdoctoral Innovation Foundation (No. 201701016), supported by SDUST Research Fund (NO. 2015JQJH104), Qingdao Postdoctoral Research funded project and National Natural Science Foundation of China (No. 51305242).

REFERENCES

Brian, P., R. D. Flack, and L. E. Barrett, (2001). Test results for a highly preloaded three-lobe journal bearing - effect of load orientation on static and dynamic characteristics. *Lubrication Engineering*

57(9), 23-30.

Elord, H. G., and M. L. Adams (1974). *A computer program for cavitation and starvation problems. Cavitation and Related Phenomena in Lubrication. Mechanical Engineering Publications*. New York, 37-41.

Ertuğrul, D., Cahit, K., Bıyıklıoğlu, A., and Kaleli, H. (2003). Measurement of friction force and effects of oil fortifier in engine journal bearings under dynamic loading conditions. *Tribology International 36*(8), 599-607.

Kim, C. C., Walther, J. H., Klit, P., and Vølund A.(2017). Investigation of journal orbit and flow pattern in a dynamically loaded journal bearing. *Tribology International 114*, 450-457.

Li, K., J. Liu, X. Han, C. Jiang, and H. Qin (2016). Identification of oil-film coefficients for a rotor-journal bearing system based on equivalent load reconstruction. *Tribology International 104*, 285-293.

Ma, Y. Y, and X. H. Cheng (2006). The cavitation erosion damage process of dynamically loaded journal bearings. Frontiers of Mechanical Engineering in China 1(4), 461-464.

Ma, Y. Y., W. H. Wang, and X. H. Cheng (2004). A Study of dynamically loaded journal bearings lubricated with non-Newtonian couple stress fluids. *Tribology Letters 17*(1), 69-74.

Osman, T. A. (2014). Effect of lubricant non-Newtonian behavior and elastic deformation on the dynamic performance of finite journal plastic bearings. *Tribology Letters 17*(1), 31-40.

Pan, J. J., H. Su, X. J. Wang, and Z. M. Zhang (2005). The analysis of the performance of dynamically loaded journal bearing with mass-conserving boundary condition. *Lubrication Engineering* (2), 41-43.

Sawicki Jerzy, T. (2005). Cavitation Effects on the Dynamics of Journal Bearings. *Applied Meehanies and Engineering 10*(3), 515-526.

Shao, K., C. W. Liu, F. R. Bi, D. Lu, and J. Zhang (2015). Analysis of hydrodynamic loads on performance characteristics of engine main bearings. Proceedings of the Institution of Mechanical Engineers, Part J: *Journal of Engineering Tribology 229*(6), 667-676.

Su, H. (2003). *Film cavitation study with the mass conserving boundary condition*. M. A. thesis, Shanghai University, Shang Hai, China.

Wang, X. L., J. Y. Zhang, and H. Dong (2011). Analysis of bearing lubrication under dynamic loading considering micropolar and cavitating effects. *Tribology International* (44), 1071-1075.

Wang, X. L., K. Q. Zhu, and S. Z. Wen (2002). On the performance of dynamically loaded journal bearings lubricated with couple stress fluids. *Tribology International 35*(3), 185-191.

Yan, K., Y. Wang, and Y. Zhu, J. Hong, and Q. Zhai (2016). Investigation on heat dissipation characteristic of ball bearing cage and inside cavity at ultra high rotation speed. *Tribology International 93*, 470-481.

Yu, B., and J. T. Sawicki (2002). Comparison of mobility method and mass conservation method in a study of dynamically loaded journal bearings. *International Journal of Rotating Machinery 8*(1), 71-79.

Zhang, C., J. X. Jiang, and H. S. Cheng (2000). A study of dynamically loaded finite journal bearings in mixed lubrication using a transient thermohydrodynamic analysis. *Tribology Transactions 43*(3), 459-464.